2019

The Effects of Matrix Metalloproteinase-9 on CX3CL1 Shedding and Axon Retraction

Lauren A. Dobrie
University of Central Florida

THE EFFECTS OF MATRIX METTALOPROTEINASE-9 ON CX3CL1 SHEDDING AND AXON RETRACTION

by

LAUREN A. DOBRIE

A thesis submitted in partial fulfillment of the requirements
for the Honors in the Major Program in Biomedical Sciences
in the College of Medicine
and the Burnett Honors College
at the University of Central Florida
Orlando, Florida

Spring Term, 2019

Thesis Chair: Alicia Hawthorne, PhD

ABSTRACT

Spinal cord injury (SCI) often leads to irreversible damage, and permanent paralysis inferior to the injury is common (Leibinger et al., 2013). Injury to the spinal cord occurs in two phases. In the first phase, components of the spinal cord are subject to mechanical trauma causing direct damage. In the second phase, damage spreads from the area of injury through molecular processes. Several studies have linked M1 "pro-inflammatory" macrophages to exacerbation of damage by inducing dieback of dystrophic axons, but not healthy axons, through direct cellular contact. Several studies have identified the presence of macrophage subtypes at specific time. A literature review was conducted in order to summarize these findings (Busch, Horn, Silver, & Silver, 2009; Evans et al., 2014; Horn, Busch, Hawthorne, van Rooijen, & Silver, 2008; Kigerl et al., 2009; Shechter et al., 2013)**.** Although the full mechanism behind the process of M1 macrophage-mediated dieback of dystrophic axons is unclear, matrix metalloproteinase-9 (MMP-9) produced by these macrophages has been shown to play a role. However, the specific interaction between MMP-9 and neurons is under investigation. The research described explores the relationship between MMP-9 and fractalkine (CX3CL1), a surface protein expressed by CNS neurons. SDS-PAGE and western blot were used to determine whether the presence of MMP-9 increases the cleavage of fractalkine at several time intervals. At a concentration of 300ng/ml, MMP-9 was not found to demonstrate cleavage of fractalkine.

ACKNOWLEDGEMENTS

I would like to extend my deepest gratitude to Nicole Verity and Katrina Pham, who have time and again gone out of their way to help me. I would also like to express my gratitude for the efforts of Dr. Robert Borgon and Dr. Emily Bradshaw while participating on my thesis committee. I would like to thank my parents for their support during this endeavor. Most of all, I would like to recognize and thank my thesis chair, Dr. Alicia Hawthorne, for being an exceptional role model and providing invaluable guidance.

TABLE OF CONTENTS

LIST OF TABLES

LIST OF FIGURES

LIST OF ABBREVIATIONS

SCI- Spinal Cord Injury

MMP-9- Matrix Metalloproteinase-9

CNS- Central Nervous System

SDS-PAGE- Sodium Dodecyl Sulfate Polyacrylamide Gel Electrophoresis

BBB- Blood Brain Barrier

ECM- Extracellular Matrix

HDAC- Histone Deacetylase

CSPG- Chondroitin Sulfate Proteoglycan

LPS- Lipopolysaccharide

INFγ- Interferon Gamma

IL- Interleukin

MCM- Macrophage Conditioned Media

CAM- Cell Adhesion Molecule

HBSS- Hank's Balanced Salt Solution

BACKGROUND

Spinal Cord Injury and Barriers to Growth

Spinal cord injury (SCI) often leads to irreversible damage, and permanent paralysis inferior to the injury is common (Leibinger et al., 2013). Injury to the spinal cord occurs in two phases. In the first phase, components of the spinal cord are subject to mechanical trauma causing direct damage. In the second phase, damage spreads from the area of injury through molecular processes. Increased blood brain barrier (BBB) permeability, inflammation, and the presence of other factors in the extracellular matrix (ECM) disrupt the microenvironment and increase damage. By this process, axonal retraction and cell death occurs not only in neurons subjected to the initial damage, but also to neurons in the surrounding areas (Donnelly & Popovich, 2008; Garcia, Aguilar-Cevallos, Silva-Garcia, & Ibarra, 2016).

When approaching the problem of axon regeneration in severed neurons, internal and external factors must be considered. Intrinsically, adult mammalian neurons show little plasticity in comparison to embryonic neurons. Differences in expression patterns hinder growth in mature cells; these differences have many causes, such as epigenetic regulation through histone acetylation. In fact, several experimental drugs targeting histone deacetylases (HDACs) have shown success in promoting neuron growth during pre-clinical trials. Inhibiting HDACs to favor acetylation of certain histone tails allows growth-promoting genes to be more accessible for transcription (Ganai, Ramadoss, & Mahadevan, 2016).

Extrinsically, a major barrier to axon regeneration after spinal cord injury is the glial scar, formed primarily by astrocytes upon CNS damage and breach of the blood brain barrier. The glial scar benefits damaged tissue by segregating it and preventing further damage, but it is a

large obstacle to successful repair. Not only does the glial scar present a physical barrier to growth, but it also contains inhibitory components such as proteoglycans (Silver & Miller, 2004). Proteoglycans, such as chondroitin sulfate proteoglycans (CSPGs), are found in highest concentrations at the epicenter of the injury. Neurons are able to grow in the presence of proteoglycans until the concentration becomes too high, at which point growth is halted (Tom, Steinmetz, Miller, Doller, & Silver, 2004). *In vitro* studies have shown success in promoting neurite outgrowth through enzymatic cleavage of proteoglycan side chains, although this growth-promoting effect is reduced in the absence of growth factors (Kigerl et al., 2009; Silver & Miller, 2004). Regeneration capabilities are regulated by a complex network of interactions among growth factors, inhibitors, ECM, and neuronal expression profiles. Expanding current knowledge about these interactions is crucial to developing new treatments for SCI.

Degeneration and Regeneration of Axons

At the site of injury, both neurite length and the growth cone shape are indicative of the state of neuron growth. In the environment of the glial scar, growth cones become dystrophic when a certain concentration of inhibitory molecules is reached. Described by Ramon y Cajal as "sterile clubs" due to their irregular shape, dystrophic end bulbs lose their ability to extend (Silver & Miller, 2004). Although they do not appear to be growing, it is interesting that these ends are constantly turning over their membrane. The lack of linear growth is not permanent, however; experimentally, neurons transferred from an inhibitory to a growth-promoting environment are able to begin growth once more (Silver & Miller, 2004; Tom et al., 2004).

In adult mammalian neurons, axotomy will not normally result in apoptosis if the cut site is far enough from the soma. When a neuron is severed at an appropriate distance, an influx of

calcium propagates from the site of axon damage to the soma. This influx leads first to growth cone collapse, followed by a latency period (Kilinc et al., 2011). Activation of several enzymes, including calpain and HDACs, leads to disassembly of the cytoskeleton. (Ganai et al., 2016; Kilinc et al., 2011). This Wallerian degeneration, characterized by the cytoskeleton disassembly distal to the axotomy site and phagocytosis of axonal fragments by glial cells and macrophages, proceeds in an anterograde fashion. In uninjured neurons, a phenomenon known as dieback may occur by a similar process in response to environmental factors or disease states, usually in a retrograde fashion (Kilinc et al., 2011).

For a short time after injury, the shortened axonal end, or "dystrophic endbulb," will attempt to sprout and regenerate (Evans et al., 2014). However, the extracellular environment is largely inhibitory and poses several obstacles to sprouting. After Wallerian degeneration and formation of dystrophic endbulbs in the first few hours after injury, dieback occurs, during which axons are retracted toward the soma (Busch et al., 2009). Studies indicate that although the initial retraction is due to intrinsic mechanisms, there is a secondary retraction phase likely mediated by direct cellular contact with blood-derived macrophages approximately 4 to 7 days post-injury (Busch et al., 2009; Evans et al., 2014).

The Role of Microglia and Blood-Derived Macrophages

Microglia residing in the central nervous system function in local immunity, synaptic maintenance, and phagocytosis of debris (Smith, Hagberg, Naylor, & Mallard, 2014). After SCI, microglia react immediately to damage (Evans et al., 2014). After approximately 3-4 days, blood-derived macrophages infiltrate the site of injury (Garcia et al., 2016; Shechter et al., 2013). Both microglia and macrophages can exist as two different varieties. The M1 variety is

considered “pro-inflammatory” and has been shown to inhibit neurogenesis, while the M2 variety is considered “anti-inflammatory” and promotes neurogenesis (Smith et al., 2014). M1 macrophages are “classically activated” by molecules such as lipopolysaccharide (LPS) and interferon-γ (INFγ). M1 cells promote inflammation by releasing inflammatory cytokines and also produce oxidative molecules, which are effective when fighting infection and tumor cells but cause incidental damage to CNS tissue (Kigerl et al., 2009). Blood-derived monocytes that differentiate into M1 cells have experimentally been shown to extravasate through the spinal cord meninges at the site of injury, in contrast to those destined to be M2 cells that enter the CSF through the choroid plexus and migrate to the injury (Shechter et al., 2013). These M2 macrophages are activated by cytokines such as IL-4 and IL-13 and promote tissue regrowth and extracellular matrix remodeling (Kigerl et al., 2009).

In typical injuries outside of the CNS, M1 cells enter the site of injury first to remove debris and induce apoptosis in damaged cells, followed by M2 cells that promote tissue regeneration and healing. In the CNS, this order is thought to be reversed, with M2 cells acting before being overwhelmed by M1 cells approximately 7 days post-injury. Several studies have used cell surface markers to track the dominance of each phenotype after SCI. The ratio of M1 to M2 cells significantly increases 7 days post-injury. It is thought that the microenvironment of the injury is responsible for this continuously elevated ratio. In one study, M2 macrophages were introduced into healthy and injured CNS tissue, and the M2 phenotype remained present only in the healthy tissue. It has been suggested that the high density of pro-inflammatory signals related to the injury, such as INFγ, are highly supportive of M1 differentiation and not M2 differentiation (Kigerl et al., 2009; Smith et al., 2014).

It is also important to note the differences in macrophage recruitment to sites of injury in the brain and spinal cord. Although the relationship between neurons and macrophages can often be generalized, the role of macrophages is different in the brain and the spinal cord. In comparison to brain injury, recruitment of macrophages is much higher in SCI. Similarly, when pro-inflammatory cytokines were introduced to both the brain and the spinal cord in the absence of injury, it was found that more macrophages were recruited to the spinal cord. Furthermore, injection of the same inflammatory cytokine to both the brain and the spinal cord does not necessarily elicit recruitment of the same white blood cell variety to both sites (Donnelly & Popovich, 2008).

Aside from the effects macrophages have on glia at the site of injury, several recent studies have focused on the direct effects they may have on neurons. The patterns of axonal growth in the presence of M1 and M2 cells are quite different. Neurons *in vitro* introduced to M2 macrophage-conditioned media (MCM) grew linearly for long distances, even in the presence of inhibitors such as CSPGs and myelin-associated glycoproteins. In contrast, those grown on M1 MCM sprouted axons that were short and branched (Kigerl et al., 2009). Not only do M1 macrophages limit growth, but direct contact with neurons may also induce dieback in dystrophic axons (Busch et al., 2009; Evans et al., 2014; Horn et al., 2008; Kigerl et al., 2009).

There are several theories surrounding the neuroprotective role of M2 macrophages. M2 cells are able to remove debris without causing damage to their surroundings via their CD206 receptors. *In vitro*, upregulation of Arginase I in M2 cells leads to synthesis of polyamines that allow neurons to grow despite myelin inhibition (Kigerl et al., 2009). The anti-inflammatory cytokines secreted by M2 cells may also benefit neuronal health. In low doses, IL-4 and IL-10

have enhanced survival of severed nerves through STAT6 and STAT3 signaling, respectively (Vidal, Lemmens, Dooley, & Hendrix, 2013).

The mechanism by which M1 cells inhibit growth is also under investigation. As stated previously, oxidative molecules produced by M1 cells, including nitric oxide radicals, are damaging to CNS tissues (Kigerl et al., 2009). Interestingly, some inflammatory cytokines produced by M1 macrophages, such as IL-6, promote high levels of linear growth. *In vitro* growth of neurons in the presence of IL-6 resulted in higher survival rates than controls and longer growth at increasing concentrations. These neurons even grew in the presence of inhibition by CNS myelin extract (Leibinger et al., 2013). Data suggests that activation of the gp130 receptor via IL-6 leads to activation of the STAT3 and P13K/Akt pathways, which are highly growth-promoting. Conversely, inhibition of IL-6 has been shown to decrease growth. However, the effects of IL-6 activation of glial cells in the CNS ultimately leads to neuronal damage (Donnelly & Popovich, 2008; Leibinger et al., 2013). This illustrates the complications that may arise when attempting to selectively alter the immune system to enhance neuronal growth, as a system is more than the sum of its parts.

M1 macrophages have also been shown to induce a secondary phase of dieback of axons through direct contact with dystrophic end bulbs. Experimental depletion of blood-derived macrophages significantly reduced secondary phase dieback *in vivo* (Horn et al., 2008). Furthermore, treatment of macrophages with trypsin prior to exposure to neurons also decreased axon dieback, while treatment with MCM did not induce dieback. This data indicates that tethering contact is necessary for macrophages to induce dieback of dystrophic axons (Horn et al., 2008). Interestingly, blood monocyte-derived M1 macrophages seem to cause this dieback

nearly 100% of the time after contact, while microglia rarely have the same effect (Evans et al., 2014; Horn et al., 2008). M1 cells possess the zinc-dependent metalloproteinase MMP-9, which is thought to be involved in axon dieback induced through cellular contact. Downregulation and inhibition of MMP-9 have been used to decrease dieback *in vivo* and *in vitro*. Metalloproteinase inhibition via GM6001 significantly reduced retraction during cellular contact. Inhibitors specific to MMP-9 such as minocycline had a similar effect in reducing dieback. This is in contrast to the inhibition of MMP-2 produced by M2 macrophages, which had no effect on dieback. MMP-9 has been a target for several new drugs used to treat spinal cord injury, including the FDA-approved methylprednisolone which suppresses MMP-9 (Busch et al., 2009). Administration of TGFα and IL-10 *in vivo* to downregulate MMP-9 were also beneficial to neuron growth (Garcia et al., 2016). Whether MMP-9 is directly involved in M1 contact with neurons or it simply contributes to the mechanism, it is apparent that the metalloproteinase is a key component in macrophage-mediated dieback of dystrophic axons after spinal cord injury.

MMP-9 and Membrane Proteins

The effects of MMP-9 on neuron growth has been successfully linked to interactions with β1 integrins *in vitro* and *in vivo*. While treatment with MMP-9 did not alter the transcriptional expression of β1 integrin mRNA, western blot assay showed that exposure to MMP-9 significantly decreased the protein amounts in cells over time (Kim et al., 2009). The data from this study suggests that MMP-9 is involved in direct cleavage of β1 integrins, destabilizing neuronal interactions with the extracellular matrix. Furthermore, decreased interactions between integrins and the extracellular matrix may lead to a decrease in intracellular

signaling via the P13K/Akt pathway (Kim et al., 2009). Cleavage of β1 integrins would promote apoptosis and inhibit adhesion to the ECM.

Matrix metalloproteinases are thought also to interact with other transmembrane adhesion molecules, including several classes of integrins, cadherins, and cell adhesion molecules (CAM). In one study, neural cell adhesion molecule (NCAM) was suggested as a substrate of MMP-9, and MMP-9 proteolytic activity was linked to exacerbation of damage after ischemic injury (Shichi, Fujita-Hamabe, Harada, & Mizoguchi, 2011). In another study, MMP-7 was shown to cleave N-cadherin, while MMP-2 showed no significant cleavage (Conant et al., 2017). N-cadherin, a type I cadherin involved in cell-to-cell adherence, was also shown to be shed from smooth muscle in response to the presence of MMP-9 (Dwivedi, Slater, & George, 2009).

Fractalkine (CX3CL1) is a chemokine commonly found on the surface of CNS neurons, but not in peripheral blood. According to Poniatowski et al., CX3CL1 is found throughout the CNS, most notably in the brain and in the dorsal horn of the spinal cord. Expression levels have been shown to vary with age as well as with certain pathological conditions (Poniatowski et al., 2017). Its receptor, CX3CR1, is commonly found on macrophages, and can also be expressed on CNS neurons (Bazan et al., 1997; Horn et al., 2008). The mature, transmembrane form of CX3CL1 contains 373 amino acid residues with up to 26 O-glycosylations. At the N-terminal domain, residues 1-76 form a chemokine domain. The chemokine domain is bound to a transmembrane domain by a mucin stalk, with a dibasic cleavage site present just before the transmembrane domain. Finally, 37 residues form the intracellular C-terminal domain (Bazan et al., 1997).

The molecular weight of fractalkine is difficult to pinpoint. One study claims the mature protein has a molecular weight of approximately 17.5kDa, but can be found at molecular weights up to 95kDa after glycosylation (Poniatowski et al., 2017). Another study found bands on western blot corresponding to fractalkine at ~100kDa, ~95kDa, and ~85kDa. The study suggested that the ~100kDa fragment corresponded to the full transmembrane form of the protein, the ~95kDa fragment corresponded to the recycled form of the transmembrane protein, and the ~85kDa fragment corresponded to the cleaved soluble chemokine domain (Zieger, Ahnelt, & Uhrin, 2014). This soluble chemokine fragment was found to have relative molecular weight of 95kDa in other studies (Bazan et al., 1997). Cleavage fragments may be produced experimentally, but they are also naturally produced by metalloproteinases such as ADAM10 and ADAM17 expressed by neurons (Dean & Overall, 2007; Poniatowski et al., 2017). The variability among these studies could be due to differences in cell types and experimental conditions (Zieger et al., 2014). However, each of these studies show that fractalkine can be found at a wide range of molecular weights due to glycosylations and natural cleavage by proteases.

The membrane-bound form of CX3CL1 acts as an adhesion molecule for monocytes. Membrane-bound CX3CL1 can be cleaved by certain enzymes, including MMP-2, to form a soluble chemokine fragment, which acts as a chemoattractant for monocytes and other leukocytes (Dean & Overall, 2007). It has been postulated that the equilibrium between the cleaved and transmembrane forms directly impacts neuron growth and survival (Zieger et al., 2014). However, the fragment has experimentally been shown to be subject to truncation by MMPs, specifically MMP-2. This truncation alters the function of the chemokine and may even

transform it into an antagonist to its own receptor, CX3CR1, thereby reducing inflammation (Dean & Overall, 2007). From this data, it is likely that MMP-9 could also induce fractalkine shedding and perhaps cleave the protein in another pattern that produces pro-inflammatory fragments. The research described in this study seeks to determine whether MMP-9 cleaves fractalkine on the surface of F11 neurons.

METHODS

Literature Review

A search of PubMed was conducted using keywords such as *M1, macrophage, inflammation, spinal cord injury,* and *axon retraction*. Studies were screened for relevance to the topic by reviewing abstracts. All irrelevant studies, as well as studies not available in English, were not included. Five studies were selected for review (Busch et al., 2009; Evans et al., 2014; Horn et al., 2008; Kigerl et al., 2009; Shechter et al., 2013). Findings concerning macrophage subtype gene expression and axon retraction timing after spinal cord injury were collected and summarized.

Sterile Cell Culture

The F11 (ECACC08062601) neuronal cell line was a generous gift from Dr. Jeff Twiss (University of South Carolina). The F11 cell line is a hybrid derived from rat embryonic DRG and mouse neuroblastoma N18TG2 cell lines. Subcultured cells are grown in DMEM/1%Penicillin-Streptomysin/10% Fetal Bovine Serum on 100mm tissue culture dishes in an incubator at 37ºC and 5% CO_2. Cultures are passaged at 70-80% confluence. Cells are washed using warmed Hank's Balanced Salt Solution (HBSS) prior to dissociation, and dissociated with 0.25% trypsin/EDTA/0.5% CO_2 warmed to 37ºC. Cells are centrifuged in new growth medium at 2,000rpm for 5 minutes, then resuspended in growth medium once more before plating. The new culture should be diluted to approximately 2-4x10,000cells/cm^2.

Treatment with MMP-9

Active human recombinant MMP-9 (EC 3.4.24.35) was purchased from Sigma-Aldrich. Prior to experimentation, the enzyme was reconstituted in sterile DMSO to a final concentration

of 0.005μg/μl. Cells were plated three days prior to experimentation on 35mm tissue culture plates in Neurobasal-A/0.5mM Glutamax/1% B27/1% Penicillin-Streptomycin. This serum-free media allowed the F11 cells to differentiate. Forskolin was added at the time of plating to aid in neuron differentiation. On day four, pictures were taken using unfiltered light microscopy in order to analyze the length and branching of neurites. The media was removed, and 1.5ml of new media containing MMP-9 (or DMSO vehicle) was added to each experimental plate as shown below, so that 300 ng of MMP-9 was present in every milliliter of media. Since MMP-9 is used at a concentration of 0.005 ug/ul, 6ul of reconstituted MMP-9 or vehicle should be added for each 1ml of media. Plates were incubated at 37ºC for 2 hours, 6 hours, or 24 hours before the protein is collected from the plates (Figure 1). These time points should be sufficient to allow cleavage to occur, as cleavage of fractalkine has been measured at 3 hours and 48 hours in the past (Dean & Overall, 2007).

Plate	MMP-9	DMSO	Incubation time (hours)
1A	-	+	2
1B	+	-	2
2A	-	+	6
2B	+	-	6
3A	-	+	24
3B	+	-	24

Table 1: Treatment and incubation times for experimental tissue culture plates

Cell Lysis, Protein Collection, and Quantification

After treatment and appropriate incubation time, the plates were placed on ice and media was collected from each of the plates into microfuge tubes. Protease inhibitor was added to the collected media. The plates were washed with cold 1X PBS before cold lysis buffer (50mM Tris-HCl, pH7.5, 40 mM NaCl, 1mM EDTA, 0.5% Triton-X, 1X protease inhibitor) was added. Cells were removed using a cell scraper, and pipetted up-and-down to ensure complete lysis. The samples were separated via microcentrifuge for 20 minutes at 4ºC at max g. The supernatant was collected, and protein quantification of the supernatant was performed using Bradford assay measured via microplate reader. Samples are added to 2X Laemmli buffer (purchased from Bio-rad), then normalized using 1X Laemmli buffer, so that at least 20ug of protein will be added to each lane on SDS-PAGE in a maximum of 25ul. Samples are then heat blocked for 5 minutes at 95ºC, mixed by vortex, and frozen at -20ºC.

Western Blot Assay

Proteins were separated via SDS-PAGE on a 1 mm 12% polyacrylamide gel. After electrophoresis, bands were western transferred to a nitrocellulose membrane using standard protocol. The membrane was blocked with BLOTTO (5% non-fat milk in TBS-T) for one hour, then treated with primary antibody dissolved in BLOTTO. The primary antibody, used at 1:1,000, is polyclonal rabbit IgG that targets the N-terminal chemokine domain of fractalkine (14-7986-81; ThermoFisher). Monoclonal mouse antibody was used at a concentration of 1:1,000 to target beta tubulin III as a loading control (T5076; Sigma). The membrane was washed and rinsed, then incubated with fluorescent secondary antibodies. Goat anti-rabbit IgG StarBright Blue 700 was added at a concentration of 1:2,500 (12004161; BioRad), and goat anti-

mouse IgG DyLight800 was added at a concentration of 1:10,000 (STAR117D800GA; BioRad). Results were visualized using ChemiDoc (BioRad), and the program ImageJ was used to quantify the amount of protein in the resulting bands (Schindelin et al., 2012). This experimental protocol was completed three times to confirm results. Cleavage fragments were expected to be visualized on western blot as indicators of increased fractalkine cleavage by MMP-9 (Conant et al., 2017). A summary of this experimental protocol is shown in Figure 1.

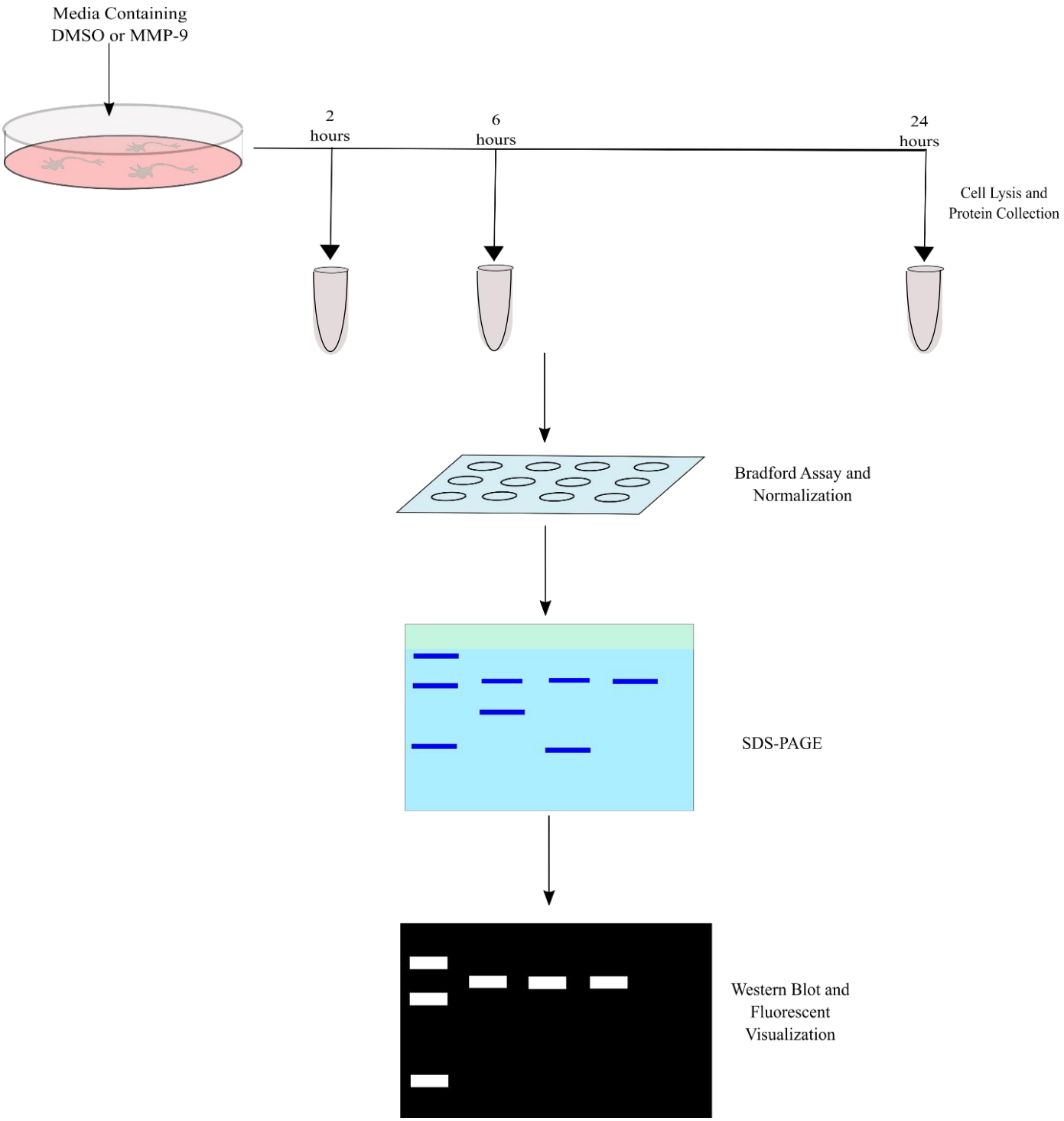

Figure 1: Diagram of Experimental Method

RESULTS

A Review of Macrophage Infiltration After Spinal Cord Injury

Five studies concerning the timing of macrophage infiltration of the spinal cord were selected for review (Busch et al., 2009; Evans et al., 2014; Horn et al., 2008; Kigerl et al., 2009; Shechter et al., 2013). These sources have gathered data showing temporal changes in expression of macrophage-specific markers, roughly summarized in Table 2. Most studies note a significant increase in blood-derived macrophages between 3 and 5 days post-injury and show that these levels remain elevated for almost a month after injury. ED-1, a general marker for macrophages, was found to be elevated from baseline on day 7, 14, and 28 post-injury, but not at 2 days post injury (Busch et al., 2009; Horn et al., 2008). Evans et al. (2014) found CX3CR1+ cells at levels elevated from baseline at 2, 5, and 8 days post injury, and observed that the number of blood-derived macrophages begins to increase rapidly 2 hours after injury. The cells reportedly increased three fold from day 0-2 and 7 fold from day 0-8 (Evans et al., 2014).

However, there is conflicting evidence related to the difference in M2 and M1 expression levels over time. For example, Kigerl et al. (2009) finds that most M1 markers are elevated on day 7 and remain elevated for up to 28 days post injury. However, iNOS was found to be elevated on day 1 and day 3 only. Furthermore, M2 markers CD206 and Arg I were found at elevated levels at completely different times. Nevertheless, the observed ratio of M1 to M2 macrophages reportedly remained equal for the first week after injury but sharply increased on day 7 post injury. Shechter et al. (2013) found that cells expressing high levels of Ly6c, an M1 marker, was elevated from day 1 through day 7, but declined by day 14. This study also found elevated levels of M2 markers longer after spinal cord injury than M1 markers. Cells expressing

high CX3CR1 and low Ly6c, characteristic of M2 macrophages, were observed at elevated levels on day 3 and remained elevated through day 14.

Using a limited number of markers to differentiate between M1 and M2 macrophages does not paint an accurate picture of the process of macrophage infiltration. One study found that a small percentage of macrophages expressed both M1 and M2 markers, suggesting that perhaps some conversion process was occurring (Evans et al., 2014). The infiltration process is highly dynamic and difficult to summarize.

Most studies noted the most significant axon retraction occurring on days 2-7 post injury, while also noting that retraction occurred up to 28 days post injury (Busch et al., 2009; Evans et al., 2014; Horn et al., 2008). Day 2 is likely when the first phase of dieback occurs, as noted by Horn et al. After day 2, the second phase of retraction begins, during which macrophages play a larger role. In fact, when macrophages were depleted, significantly less dieback occurred on days 4 and 7 compared to control (Horn et al., 2008). During the second phase, some studies report that cellular contact with macrophages induced dieback 100% of the time, and no dieback was observed without cellular contact with macrophages (Busch et al., 2009; Evans et al., 2014; Horn et al., 2008). However, Evans et al. also noted that the number of non-destructive contacts was greater than the number of destructive contacts on all days post-injury. In other words, the number of contacts between macrophages and axons that resulted in dieback was significantly fewer than those that did not result in dieback after spinal cord injury.

			Days Post-Injury								
Reference	Animal Model	Macrophage-Specific Marker	1	2	3	4	5	7	8	14	28
(Busch et al., 2009)	Rat SCI	ED-1		-		↑		↑		↑	↑
(Horn et al., 2008)	Rat SCI	ED-1		-		-		↑		↑	↑
(Evans et al., 2014)	Rat SCI	CX3CR1		↑			↑		↑		
		CD11b					↑				
(Kigerl et al., 2009)	Mouse SCI	CD86*	-		-			-		-	↑
		iNOS*	↑		↑			-		-	-
		CD16*	-		-			↑		↑	↑
		CD32*	-		-			↑		↑	↑
		CD206†	-		-			↑		↑	-
		Arg I†	↑		↑			-		-	-
(Shechter et al., 2013)	Mouse SCI	Ly6c (hi) *	↑		↑		↑	↑		-	
		CX3CR1 (hi)†	-		↑		↑	↑		↑	

Table 2: Summary of macrophage infiltration after spinal cord injury. This table aims to summarize the time points after spinal cord injury at which macrophage-specific markers are found at elevated levels at the area of injury compared to baseline.
↑ =increased compared to baseline; - =no significant increase from baseline; * =marker specific to M1 macrophage subtype; † =marker specific to M2 macrophage subtype

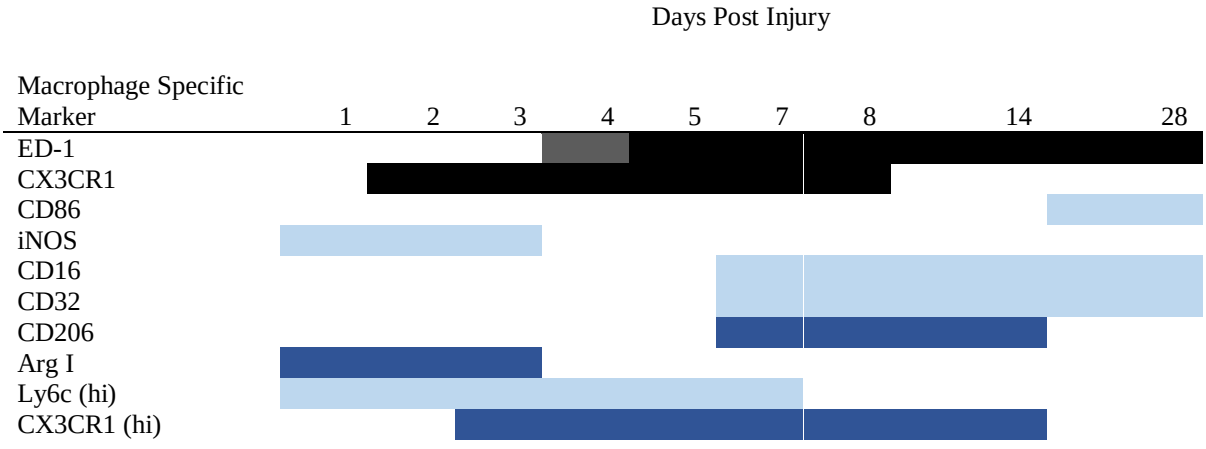

Figure 2: Graphical representation of macrophage-specific markers found at specific time intervals after spinal cord injury. Colored area reflects measurements significantly elevated from baseline. Macrophage-specific markers (black), M1 specific markers (light blue), and M2 specific markers (dark blue) are included. Gray areas reflect conflicting findings from multiple studies.

Cell Morphology

Prior to collection of protein samples, images were collected using light microscopy to document cell morphology before and after treatment. As shown in Figure 2, there were no dramatic changes observed in soma or neurite morphology after treatment with MMP-9 or vehicle for 24 hours. F11 cells maintain long, branching neurites after treatment. These results were similar to those obtained after 2 and 6 hours of treatment.

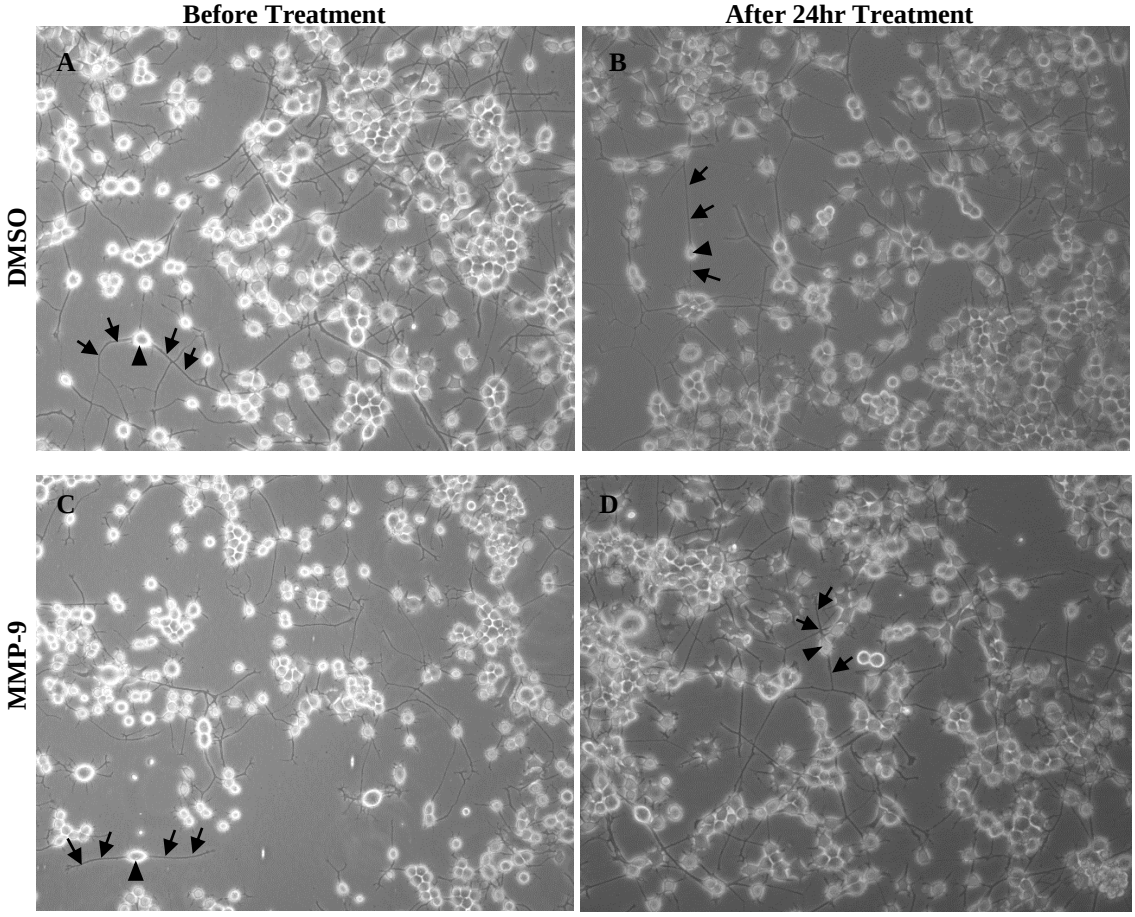

Figure 3: Light microscopy captures morphology of differentiated F11 neurons before and after 24 hours of treatment. Pictures in the top panel were taken before (A) and after (B) treatment with DMSO for 24 hours. The bottom panel images were taken before (C) and after (D) treatment with MMP-9 for 24 hours. Arrowheads indicate cell bodies, and arrows indicate neurites.

Measurement of Total Fractalkine after Western Blot

F11 neurons were grown in Neurobasal-A media containing either 300 ng/ml MMP-9 or DMSO vehicle for 2, 6, or 24 hours. Protein samples were collected at the end of each respective time interval and separated via SDS-PAGE. Proteins were transferred to a nitrocellulose membrane for western blot to detect fractalkine. Anti-β-tubulin III antibodies were included to detect β-tubulin III as a loading control. Upon observation of the resulting membranes after fluorescent visualization, it is apparent that the banding pattern of fractalkine is relatively uniform across each lane. An array of bands ranging from ~100kDa to ~17.5kDa was expected due to the multiple glycosylations typical of the protein and the natural shedding of the chemokine domain (Dean & Overall, 2007; Zieger et al., 2014). ImageJ was used to analyze the total amount of fractalkine and tubulin found in each lane. The ratio of fractalkine to tubulin was calculated for each lane in order to normalize the amount of fractalkine to the total protein loaded onto the gel based on the tubulin loading control. The mean was taken for all three trials and displayed graphically with the standard deviation (Figure 3E). An outlier was omitted from the average fractalkine after treatment with MMP-9 for 6 hours, which caused a large variability in this data point.

Anti-fractalkine antibodies targeted the extracellular portion of the protein. It was expected that if MMP-9 cleaved fractalkine, fragments would be detected in the media sample and less total fractalkine would be present in the lysate. There are no bands visible in the media lanes, and ImageJ was used to confirm the lack of fragments able to be detected. Several trends can be observed regarding the total fractalkine in the cell lysate. First, there seems to be a reduction in the total amount of fractalkine between 2 and 24 hours regardless of treatment.

Second, there is a possible reduction in total fractalkine after treatment with MMP-9 for 2 hours compared to control treatment. Finally, after 24 hours, there seems to be no difference in the total fractalkine found in the control and MMP-9 treatment groups.

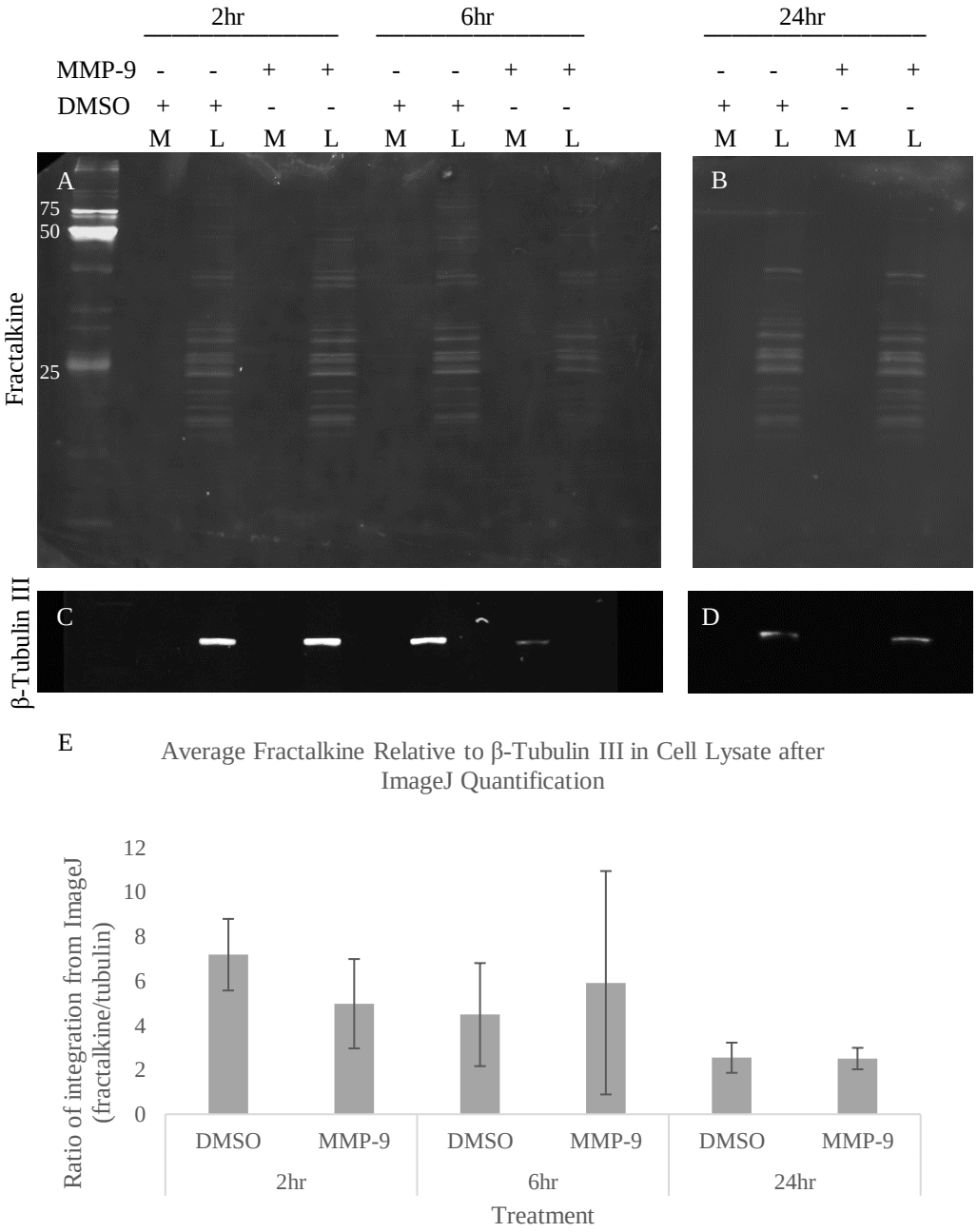

Figure 4: Western Blot Results. The collected media (M) and cell lysate (L) samples were probed using fluorescent antibodies. Exposure of the trial 1 blots at a 700 nm wavelength allows for visualization of targeted fractalkine (A,B). Exposure of the same blot at 800 nm wavelength shows targeted β-tubulin III (C,D). Bands from all trials were quantified using ImageJ, and the average ratio of fractalkine to tubulin for each condition was plotted plus or minus one standard deviation (E). After 2 hours, cells treated with DMSO had an average fractalkine/tubulin ratio of 7.179±1.611 and cells treated with MMP-9 had a ratio of 4.974±2.010. After 6 hours, cells treated with DMSO had an average ratio of 4.482±2.319 and cells treated with MMP-9 had a ratio of 5.916±5.026. After 24 hours, cells treated with DMSO had an average ratio of 2.542±0.678 and cells treated with MMP-9 had a ratio of 2.505±0.483. These results are shown graphically above (E).

DISCUSSION

After 2 hours, 6 hours, and 24 hours, there was no evidence of fractalkine fragments in the media samples collected (Figure 3). However, a trend suggests a possible decrease in fractalkine in the cell lysate after 2 hours compared to control, but not 24 hours. This could suggest that MMP-9 is only able to acutely affect fractalkine shedding. However, because the control and experimental measurements were relatively close, the data could also suggest that at a concentration of 300 ng/ml, MMP-9 has no effect on fractalkine cleavage. Due to the limited number of trials performed, it is difficult to draw many conclusions from the data obtained from western blot and imaging.

Previous studies have shown that M1 macrophages induce axon dieback through direct contact involving MMP-9 (Busch et al., 2009; Garcia et al., 2016; Horn et al., 2008). However, the full mechanism behind this is not entirely clear. N-cadherins, β1-integrins, and other proteins on the neuronal membrane have been suggested to play a role (Conant et al., 2017; Kim et al., 2009). Had fractalkine been cleaved by MMP-9 in this experiment, it could have been hypothesized that MMP-9 induces dieback in axons in part through its cleavage of fractalkine. If the results are truly negative, it can be deduced that fractalkine does not play a role in dieback directly induced by MMP-9.

If cleavage fragments were produced, it may have been an interesting extension of this experiment to observe the effect of these cleavage fragments on neuron growth. As discussed in previous sections, fractalkine is known to be cleaved by MMP-2 to produce a chemokine fragment. Further truncation by MMP-2 alters the function of the chemokine and may even transform it into an antagonist to its own receptor, CX3CR1, thereby reducing inflammation

(Dean & Overall, 2007). It is likely that MMP-9 could also induce fractalkine shedding and perhaps cleave the protein in another pattern that produces pro-inflammatory fragments. The cytokine fragments may produce a paracrine signal that exacerbates damage. Further optimization and research should be done in order to increase our understanding of the role of MMP-9 in exacerbation of spinal cord injury.

Several improvements could be made to this protocol. First and foremost, decreasing the amount of noise during fluorescent visualization of western blot could increase the accuracy of the results. Minimizing contamination, increasing blocking time, and optimizing antibody dilutions could significantly reduce noise when visualizing the blot at 700 nm. Ensuring the absence of air bubbles during western transfer could improve the accuracy of the transfer. These procedures could in turn increase the accuracy of ImageJ measurements by decreasing the noise to signal ratio. Furthermore, increasing the number of trials would allow for more effective statistical analysis of the data acquired.

Perhaps devising a way to remove glycosylations from CX3CL1 could help standardize the molecular weight of the protein and make it easier to detect cleavage. Running SDS-PAGE for a longer period of time may have allowed for better separation and visualization of larger fragments. Furthermore, if the cleavage fragments produced by MMP-9 were of an extremely small molecular weight, they may have been lost during western transfer, and optimizing this procedure may also help with visualization. It is also possible that concentrating the media samples could have allowed for better visualization of any fragments cleaved. If only a small amount of fragments were produced, the media may have been too dilute for proper visualization. Higher concentrations of MMP-9 may have also been useful. A concentration of

300 ng/ml may have been too low to produce significant changes. Finally, a positive control, such as treatment with MMP-2, may provide more insight to negative results.

WORKS CITED

Bazan, J. F., Bacon, K. B., Hardiman, G., Wang, W., Soo, K., Rossi, D., . . . Schall, T. J. (1997). A new class of membrane-bound chemokine with a CX3C motif. *Nature, 385*, 640-644. Retrieved from https://doi.org/10.1038/385640a0

doi:10.1038/385640a0

Busch, S. A., Horn, K. P., Silver, D. J., & Silver, J. (2009). Overcoming macrophage-mediated axonal dieback following CNS injury. *Journal of Neuroscience, 29*(32), 9967-9976. Retrieved from https://www.ncbi.nlm.nih.gov/pubmed/19675231

https://www.ncbi.nlm.nih.gov/pmc/PMC2771342/. doi:10.1523/JNEUROSCI.1151-09.2009

Conant, K., Daniele, S., Bozzelli, P. L., Abdi, T., Edwards, A., Szklarczyk, A., . . . Maguire-Zeiss, K. (2017). Matrix metalloproteinase activity stimulates N-cadherin shedding and the soluble N-cadherin ectodomain promotes classical microglial activation. *Journal of neuroinflammation, 14*(1), 56-56. Retrieved from https://www.ncbi.nlm.nih.gov/pubmed/28302163

https://www.ncbi.nlm.nih.gov/pmc/PMC5356362/. doi:10.1186/s12974-017-0827-4

Dean, R. A., & Overall, C. M. (2007). Proteomics Discovery of Metalloproteinase Substrates in the Cellular Context by iTRAQ™ Labeling Reveals a Diverse MMP-2 Substrate Degradome. *Molecular & Cellular Proteomics, 6*(4), 611. Retrieved from http://www.mcponline.org/content/6/4/611.abstract

http://www.mcponline.org/content/6/4/611.

Donnelly, D. J., & Popovich, P. G. (2008). Inflammation and its role in neuroprotection, axonal regeneration and functional recovery after spinal cord injury. *Experimental neurology,*

209(2), 378-388. Retrieved from http://www.sciencedirect.com/science/article/pii/S0014488607002518. doi:https://doi.org/10.1016/j.expneurol.2007.06.009

Dwivedi, A., Slater, S. C., & George, S. J. (2009). MMP-9 and -12 cause N-cadherin shedding and thereby β-catenin signalling and vascular smooth muscle cell proliferation. *Cardiovascular Research, 81*(1), 178-186. Retrieved from http://dx.doi.org/10.1093/cvr/cvn278 https://academic.oup.com/cardiovascres/article/81/1/178/277393. doi:10.1093/cvr/cvn278

Evans, T. A., Barkauskas, D. S., Myers, J. T., Hare, E. G., You, J. Q., Ransohoff, R. M., . . . Silver, J. (2014). High-resolution intravital imaging reveals that blood-derived macrophages but not resident microglia facilitate secondary axonal dieback in traumatic spinal cord injury. *Experimental neurology, 254*, 109-120. Retrieved from https://www.ncbi.nlm.nih.gov/pubmed/24468477 https://www.ncbi.nlm.nih.gov/pmc/PMC3954731/. doi:10.1016/j.expneurol.2014.01.013

Ganai, S. A., Ramadoss, M., & Mahadevan, V. (2016). Histone Deacetylase (HDAC) Inhibitors - emerging roles in neuronal memory, learning, synaptic plasticity and neural regeneration. *Current neuropharmacology, 14*(1), 55-71. Retrieved from https://www.ncbi.nlm.nih.gov/pubmed/26487502 https://www.ncbi.nlm.nih.gov/pmc/PMC4787286/. doi:10.2174/1570159X13666151021111609

Garcia, E., Aguilar-Cevallos, J., Silva-Garcia, R., & Ibarra, A. (2016). Cytokine and Growth Factor Activation In Vivo and In Vitro after Spinal Cord Injury. *Mediators of*

inflammation, 2016, 9476020-9476020. Retrieved from https://www.ncbi.nlm.nih.gov/pubmed/27418745 https://www.ncbi.nlm.nih.gov/pmc/PMC4935915/. doi:10.1155/2016/9476020

Horn, K. P., Busch, S. A., Hawthorne, A. L., van Rooijen, N., & Silver, J. (2008). Another Barrier to Regeneration in the CNS: Activated Macrophages Induce Extensive Retraction of Dystrophic Axons through Direct Physical Interactions. *The Journal of neuroscience, 28*(38), 9330. Retrieved from http://www.jneurosci.org/content/28/38/9330.abstract http://www.jneurosci.org/content/jneuro/28/38/9330.full.pdf.

Kigerl, K. A., Gensel, J. C., Ankeny, D. P., Alexander, J. K., Donnelly, D. J., & Popovich, P. G. (2009). Identification of two distinct macrophage subsets with divergent effects causing either neurotoxicity or regeneration in the injured mouse spinal cord. *Journal of Neuroscience, 29*(43), 13435-13444. Retrieved from https://www.ncbi.nlm.nih.gov/pubmed/19864556 https://www.ncbi.nlm.nih.gov/pmc/PMC2788152/. doi:10.1523/JNEUROSCI.3257-09.2009

Kilinc, D., Peyrin, J.-M., Soubeyre, V., Magnifico, S., Saias, L., Viovy, J.-L., & Brugg, B. (2011). Wallerian-like degeneration of central neurons after synchronized and geometrically registered mass axotomy in a three-compartmental microfluidic chip. *Neurotoxicity research, 19*(1), 149-161. Retrieved from https://www.ncbi.nlm.nih.gov/pubmed/20162389 https://www.ncbi.nlm.nih.gov/pmc/PMC3006648/. doi:10.1007/s12640-010-9152-8

Kim, G. W., Kim, H.-J., Cho, K.-J., Kim, H.-W., Cho, Y.-J., & Lee, B. I. (2009). The role of MMP-9 in integrin-mediated hippocampal cell death after pilocarpine-induced status

epilepticus. *Neurobiology of Disease, 36*(1), 169-180. Retrieved from http://www.sciencedirect.com/science/article/pii/S096999610900179X. doi:https://doi.org/10.1016/j.nbd.2009.07.008

Leibinger, M., Müller, A., Gobrecht, P., Diekmann, H., Andreadaki, A., & Fischer, D. (2013). Interleukin-6 contributes to CNS axon regeneration upon inflammatory stimulation. *Cell death & disease, 4*(4), e609-e609. Retrieved from https://www.ncbi.nlm.nih.gov/pubmed/23618907 https://www.ncbi.nlm.nih.gov/pmc/PMC3641349/. doi:10.1038/cddis.2013.126

Poniatowski, Ł. A., Wojdasiewicz, P., Krawczyk, M., Szukiewicz, D., Gasik, R., Kubaszewski, Ł., & Kurkowska-Jastrzębska, I. (2017). Analysis of the Role of CX3CL1 (Fractalkine) and Its Receptor CX3CR1 in Traumatic Brain and Spinal Cord Injury: Insight into Recent Advances in Actions of Neurochemokine Agents. *Molecular neurobiology*, *54*(3), 2167-2188. Retrieved from https://www.ncbi.nlm.nih.gov/pubmed/26927660 https://www.ncbi.nlm.nih.gov/pmc/PMC5355526/. doi:10.1007/s12035-016-9787-4

Schindelin, J., Arganda-Carreras, I., Frise, E., Kaynig, V., Longair, M., Pietzsch, T., . . . Cardona, A. (2012). Fiji: an open-source platform for biological-image analysis. *Nature Methods, 9*, 676. Retrieved from https://doi.org/10.1038/nmeth.2019. doi:10.1038/nmeth.2019 https://www.nature.com/articles/nmeth.2019#supplementary-information

Shechter, R., Miller, O., Yovel, G., Rosenzweig, N., London, A., Ruckh, J., . . . Schwartz, M. (2013). Recruitment of beneficial M2 macrophages to injured spinal cord is orchestrated

by remote brain choroid plexus. *Immunity, 38*(3), 555-569. Retrieved from https://www.ncbi.nlm.nih.gov/pubmed/23477737 https://www.ncbi.nlm.nih.gov/pmc/PMC4115271/. doi:10.1016/j.immuni.2013.02.012

Shichi, K., Fujita-Hamabe, W., Harada, S., & Mizoguchi, H. (2011). Involvement of Matrix Metalloproteinase-Mediated Proteolysis of Neural Cell Adhesion Molecule in the Development of Cerebral Ischemic Neuronal Damage. *Journal of Pharmacology and Experimental Therapeutics, 338*(2), 701-710. Retrieved from http://jpet.aspetjournals.org/content/jpet/338/2/701.full.pdf.

Silver, J., & Miller, J. H. (2004). Regeneration Beyond the Glial Scar. *Nature Reviews Neuroscience, 5*(2), 146-156. doi:10.1038/nrn1326

Smith, P. L. P., Hagberg, H., Naylor, A. S., & Mallard, C. (2014). Neonatal Peripheral Immune Challenge Activates Microglia and Inhibits Neurogenesis in the Developing Murine Hippocampus. *Developmental Neuroscience, 36*(2), 119-131. Retrieved from https://www.karger.com/DOI/10.1159/000359950. doi:10.1159/000359950

Tom, V. J., Steinmetz, M. P., Miller, J. H., Doller, C. M., & Silver, J. (2004). Studies on the Development and Behavior of the Dystrophic Growth Cone, the Hallmark of Regeneration Failure, in an In Vitro Model of the Glial Scar and after Spinal Cord Injury. *The Journal of neuroscience, 24*(29), 6531. Retrieved from http://www.jneurosci.org/content/24/29/6531.abstract.

Vidal, P. M., Lemmens, E., Dooley, D., & Hendrix, S. (2013). The role of "anti-inflammatory" cytokines in axon regeneration. *Cytokine & Growth Factor Reviews, 24*(1), 1-12.

Retrieved from http://www.sciencedirect.com/science/article/pii/S135961011200072X. doi:https://doi.org/10.1016/j.cytogfr.2012.08.008

Zieger, M., Ahnelt, P. K., & Uhrin, P. (2014). CX3CL1 (fractalkine) protein expression in normal and degenerating mouse retina: in vivo studies. *PloS one, 9*(9), e106562-e106562. Retrieved from https://www.ncbi.nlm.nih.gov/pubmed/25191897 https://www.ncbi.nlm.nih.gov/pmc/PMC4156323/. doi:10.1371/journal.pone.0106562